Magneto-Dielectric Composites Characterization Using Resonant Sensor and Neural Network Modeling

Germán Álvarez-Botero, *Senior Member, IEEE*, Humberto Lobato-Morales, *Senior Member, IEEE*, Katherine Hui, Naji Tarabay, Jeu Sanchez-Vargas, Camilo Velez, *Member, IEEE*, and Gabriela Méndez-Jerónimo, *Member, IEEE*

***Abstract*— This article presents a novel way to estimate magnetodielectric composites' complex permittivity (ε) and permeability (μ). A methodology based on artificial neural network (ANN) modeling is proposed to determine ε and μ from *S*-parameter measurements around 2.45 GHz, obtained using a new microstrip split ring resonator (SRR)-based resonant sensor.**

***Index Terms*— Artificial neural networks (ANNs), microwave characterization, PDMS-Fe_3O_4 composite.**

I. Introduction

ADDITIVE manufacturing has spurred interest in developing next-generation RF/microwave devices, like antennas [1], [2], filters [3], [4], or phase shifters [5], [6], with a focus on innovative materials like magneto-dielectrics (MD). To characterize MD materials and extract permittivity (ε) and permeability (μ) values, various methods involving waveguides [7], [8], [9], microstrip transmission lines, and resonant structures like split-ring resonators (SRR) have been employed [10], [11], [12], [13], [14]. However, these approaches face limitations in characterizing MD materials with non-zero complex permeability, and often use separate polynomial expressions for ε and μ, neglecting their intrinsic correlation.

This letter proposes a novel SRR sensor, and a parameter extraction procedure based on artificial neural networks (ANNs) to determine ε and μ parameters simultaneously from an MD sample. The sensor excites two sensing areas to concentrate electric and magnetic fields for a single measurement on the sample, eliminating the need to relocate the sample-under-test (SUT) and reducing associated errors. The ANN method processes the sensor output, considering the intrinsic correlation between ε and μ, thus avoiding inaccuracies from separate extraction procedures.

The proposed sensor and parameter extraction methodology are evaluated by determining ε and μ parameters for MD composite materials with varying concentrations of Fe_3O_4 nanoparticles. The results validate the usability of the proposed approach for characterizing new materials.

Manuscript received 4 January 2024; accepted 17 January 2024. Date of publication 5 February 2024; date of current version 10 April 2024. This work was supported by the Samueli School of Engineering, University of California, Irvine. *(Corresponding author: Germán Álvarez-Botero.)*

Germán Álvarez-Botero is with the Department of Electrical, Electronic and Communications Engineering, Public University of Navarre, 31006 Pamplona, Spain (e-mail: germanandres.alvarez@unavarra.es).

Humberto Lobato-Morales, Jeu Sanchez-Vargas, and Gabriela Méndez-Jerónimo are with the CICESE, Ensenada 22860, Mexico (e-mail: humbertolm@ieee.org).

Katherine Hui, Naji Tarabay, and Camilo Velez are with the Magnetic Microsystems and Microrobotics Laboratory, Mechanical and Aerospace Engineering Department, University of California, Irvine, Irvine, CA 92697 USA (e-mail: cvelezcu@uci.edu).

Color versions of one or more figures in this letter are available at https://doi.org/10.1109/LMWT.2024.3356418.

Digital Object Identifier 10.1109/LMWT.2024.3356418

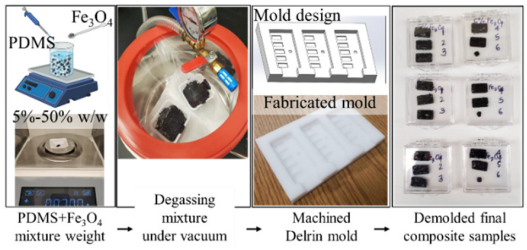

Fig. 1. Illustration of the sample fabrication procedure.

II. Magneto-Dielectric Sample Preparation and Its Magnetic Characterization

The MD composite samples used in this work are fabricated based on PDMS-silicon (*DecorRom*, *ASKU0055*) mixed with Fe_3O_4 20–30 nm nanoparticles (98% purity) from *SkySpring Nanomaterials, Inc.* [15], adapting procedures suggested in [16] and follow standard compounding techniques from pharmacy industry such as geometric dilution and levigation. The proposed weight ratio for silicone and nanoparticles is 5%, 10%, 15%, 25%, 40%, and 50% of the Fe_3O_4 nanoparticles.

A *U.S. Solid USS-DBS8* Digital Analytical Balance Scale with a resolution of 0.1 mg is used to control the weights of silicone and nanoparticles before mixing; then, they are thoroughly mixed and introduced into a vacuum chamber at -1 atm to avoid the possibility of forming air bubbles. The mixture is then spread into a *Delrin* mold previously machined using a CNC, configured for the sample dimensions of 10.5 mm length, 6 mm width, and 1 mm height. Each sample is weighted after being removed from the mold, and the actual composite proportions are calculated. Fig. 1 shows the fabrication process.

A. Magnetic Characterization

Magnetic measurements are performed using a MicroSense *VSM*(*EZ9HF VSM*), varying the excitation of the H-field up

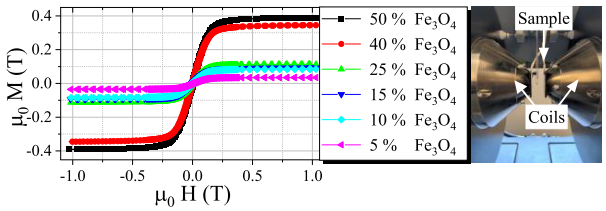

Fig. 2. Magnetization ($\mu_0 \cdot M$) versus applied external magnetic field ($\mu_0 \cdot H$) curves of the prepared PDMS-Fe_3O_4 composites.

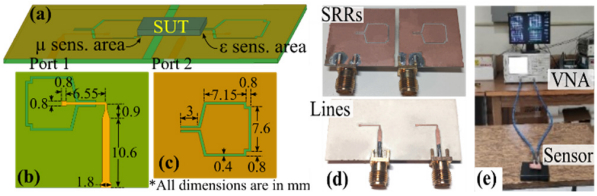

Fig. 3. Proposed planar resonant sensor for the magneto-dielectric composites characterization. (a) Perspective view. (b) Coupling-line view. and (c) SRR view. (d) Fabricated CSRRs and coupling-lines views. (e) Setup for the ε-μ composites characterization.

to 1 T at room temperature. The responses are shown in Fig. 2, and as observed, the saturation magnetization increases proportionally with the nanoparticle concentration for all the evaluated composites. By the other hand, it is observed no significant variation on the coercivity neither the magnetic susceptibility of the samples when varying the nanoparticles concentration, confirming the retention of composite's super-paramagnetic characteristics, a highly desirable condition for low-loss microwave materials [16], [17], [18], [19], [20].

Once the *MvsH*-behavior of the composites is evaluated, the estimation of their ε and μ parameters is carried out to complete the E-H material characterization. A resonant sensor having the capability of simultaneously sensing ε and μ at microwave frequencies is designed and used, as explained hereafter.

III. Planar Sensor for Simultaneously Measuring Permittivity and Permeability

Planar microwave sensors play a crucial role in researching the EM properties of materials, providing a controlled environment and a fast non-destructive way to study how materials interact with EM fields at microwave frequencies. In particular, the resonant method for the characterization of materials using microwave sensors is based on the field perturbation theory: the used sensing circuit is configured such that the electric-E (magnetic-H) field is confined to specific regions; loading of a sample in such regions causes the material ε (μ) to interact with the circuit E (H) field, leading the sensor resonant parameters, resonant frequency f_r and quality factor Q, to vary. The sample ε (μ) value is then estimated from the evaluation of the change in f_r and Q [21].

A. Design of the Planar Micro Resonant Sensor

Fig. 3(a) shows the designed circuit, which comprises two sections composed of a square-shaped SRR each, etched on the ground plane (top view); such resonators are configured to act as the sensing elements, and they are fed by open-terminated transmission lines (bottom view) by means

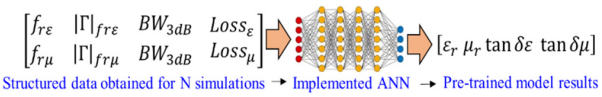

Fig. 4. Processes of the technique to determine SUT permittivity and permeability values by ANN modeling.

of proximity coupling. Each feeding line is composed of two main sections: a 50 Ω segment, and a narrower section bent 90° terminated with a small patch. The length of the narrow section is adjusted in simulations for the SRRs to be critically coupled [21], so the resonant parameters can be clearly extracted. Both SRR sections are electrically separated by a gap on the ground-plane in order to isolate them. The circuit was designed using a *Rogers*[1] *RO4003C* dielectric substrate having $\varepsilon_r = 3.55$, $\tan\delta = 0.0021$, and height $h = 0.813$ mm. [22]; *SonnetSoftware*[1] was employed to configure and tune the circuit.

As shown in Fig. 3(a), the SUT is placed over the two portions of the SRRs, configured as the SUT-ε and SUT-μ sensing areas, and are defined by a high-intensity region of the E-field produced by the first SRR, and the concentration of the H-field on the second SRR, respectively.

By employing *Ansys-HFSS* simulator, the sensing circuit and SUT are analyzed; ε_r and μ_r of the SUT are configured to vary from 1 to 10, and from 1 to 2, respectively, in steps of 0.1. Reflection responses $|S_{11}|$ and $|S_{22}|$ are obtained, and the resonant parameters f_r (resonant frequency), $|\Gamma|_{fr}$ (magnitude of reflection at f_r), BW (3-dB bandwidth), and the power loss for μ and ε sensors are extracted from each curve. Losses obtained from the ε section were calculated as $\text{Loss}_\varepsilon = 1 - |S_{11}|^2$ while those obtained for the μ were obtained as $\text{Loss}_\mu = 1 - |S_{22}|^2$ [23]. Then, these parameters extracted from EM simulations are used as training, validation, and testing data, as explained hereafter.

IV. ANN for the Magneto-Dielectric Composites Characterization

As $|S_{11}|$ and $|S_{22}|$ responses of the sensor contain information on the ε and μ of the MD composites sample, their characteristic resonant parameters f_r, $|\Gamma|_{fr}$, BW, and Losses of each corresponding pair ε–μ can be used as training parameters to implement an ANN model.

Using MATLAB,[1] an ANN model was implemented as shown in Fig. 4. It is composed of an input layer with 8 neurons (resonant parameters for the pair ε-μ of the SUT), 10 hidden layers, and an output layer with two neurons (SUT ε and μ). The training inputs are 2000 datasets obtained from the reflection coefficient responses as a function of the frequency from each sensor full-wave simulation. This dataset was divided into three subsets, taking 70% of data for training, 15% for validation, and 15% for testing. Classes for the trained model are established by ε_r, μ_r, and by the electric and magnetic loss tangents ($\tan\delta\varepsilon$, and $\tan\delta\mu$), respectively.

Under this data segmentation, the model provides a testing performance (error between the input values and the actual output values) of 0.003 in 31 epochs. Finally, the most

[1]Registered trademark.

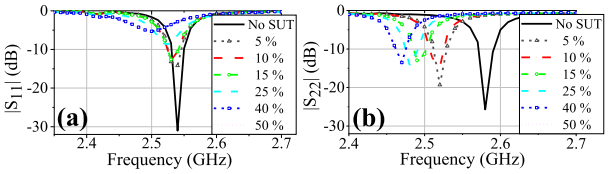

Fig. 5. Measured reflection curves of the sensor loaded with the different Fe_3O_4 concentration SUTs for calculation of (a) ε and (b) μ.

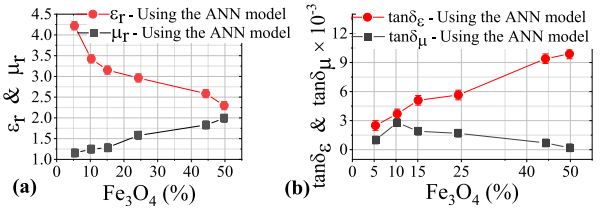

Fig. 6. Dielectric and magnetic parameter estimation of the SUTs for the different Fe_3O_4 measured concentrations: (a) ε_r and μ_r. (b) tan$\delta\varepsilon$ and tan$\delta\mu$ ($n = 3$, $m = 5$).

significant error of 0.0001 for 80 validation tests was obtained, showing an excellent correlation between the ANN model and the EM simulation.

Once the error on the ANN model is minimized, the trained model is used with the experimental data as input, obtaining ε_r, μ_r, tan$\delta\varepsilon$, and tan$\delta\mu$ for each MD sample fabricated.

V. Experimental Validation

To validate experimentally the applicability of the proposed method to characterize the MD composites, the designed sensor is fabricated by PCB milling technique. Then, two-port *S*-parameters measurements are performed from 2 to 3 GHz using an *Agilent 8753ES*-series vector network analyzer (VNA). The equipment was previously calibrated using a short-open-load-thru (SOLT) calibration procedure, establishing a reference impedance of 50 Ω. Fig. 3(d) and (e) show the fabricated sensor and the implemented setup.

To minimize potential variations in the PDMS-Fe_3O_4 mixture, three samples ($n = 3$) were fabricated for each concentration. Subsequently, *S*-parameter measurements were conducted for each set, involving five consecutive frequency sweeps ($m = 5$). The data used to determine ε and μ were derived from the averaged results of these sweeps and the average of the sample sets corresponding to the Fe_3O_4 concentration.

Fig. 5(a) and (b) show the return loss responses of the sensor for ε and μ estimation, respectively. When each prepared composite having different Fe_3O_4 concentrations is placed as SUT; measurements of the empty sensor serve as the reference data, as stated in the resonant measurement technique [21].

Subsequently, the results shown in Fig. 5 serve as input data for the proposed ANN model. This, in turn, yields the values of εr, μr, tan$\delta\varepsilon$, and tan$\delta\mu$ for the manufactured MD composites. The resulting data for each concentration of Fe_3O_4 is shown in Fig. 6(a) and (b).

Due to various mechanisms of electric and magnetic losses, such as hysteresis loss, dielectric loss, and residual loss, ε_r and μ_r of the MD materials are complex-valued [24], i.e., $\varepsilon_r = \varepsilon_r'(1 - j\tan\delta_\varepsilon)$ and $\mu_r = \mu_r'(1 - j\tan\delta_\mu)$, where ε_r' and μ_r' are the real parts of the ε and μ.

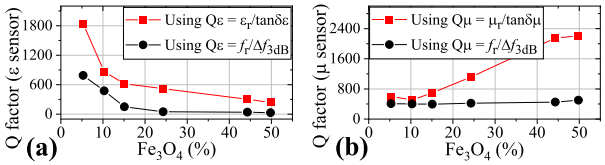

Fig. 7. Comparison of the Q factor obtained from a single point resonant method ($Q = f_r/\Delta f_{3dB}$) and calculated using intrinsic parameters from the proposed ANN modeling for (a) ε sensor and (b) μ sensor ($n = 3$, $m = 5$).

TABLE I
Comparison With Previous Works

Reference	ε_r	tan$\delta\varepsilon$	μ_r	tan$\delta\mu$	ANN	Q-fact.
[14]	✓	✓	×	×	×	×
[11]	✓	×	✓	×	×	×
[26]	✓	×	✓	×	×	×
[10]	✓	✓	✓	✓	×	×
This work	✓	✓	✓	✓	✓	✓

Losses in resonant sensors are quantified by the quality factor (Q), Usually determined as $Q = f_r/\Delta f_{3dB}$, where f_r is the resonant frequency and Δf_{3dB} is the 3-dB bandwidth. It is important to note that this method to determine Q is applicable to resonators with a single resonant point with a simple *R–L–C* or *G–L–C* equivalent circuit [25]. However, when the SUT is placed in the sensor, multiple resonant points appear, superposing and affecting the 3-dB values of the particular resonance, leading to inaccuracies in Q calculation, especially for low Q responses, as observed when the Fe_3O_4 concentration increases, as shown in Fig. 5.

Therefore, to accurately determine the Q factor of the evaluated MD composites, it is necessary to consider the intrinsic relationship between ε_r, μ_r, tan$\delta\varepsilon$, and tan$\delta\mu$, as provided by the proposed ANN model. Thus, Q factor can be calculated from the intrinsic properties of the material as $Q\varepsilon = \varepsilon_r/\tan\delta\varepsilon$ and $Q\mu = \mu_r/\tan\delta\mu$. The results obtained using this expression are shown in Fig. 7.

Compared to previous studies, the proposed method enables the systematic extraction of ε_r, μ_r, tan$\delta\varepsilon$, and tan$\delta\mu$ from an ANN model. This model considers the intrinsic relationship between ε and μ, allowing for the quantification of losses in MD composites. This approach helps to avoid underestimation issues that arise when using the single-point resonant method to obtain the Q factor in low resonant sensor responses. A summary of the findings is presented in Table I.

VI. Conclusion

An innovative machine learning-based method was introduced to determine complex ε and μ, demonstrating its effectiveness in assessing the fabrication process of MD composites. The studied MD material exhibited low magnetic hysteresis and a high electric and magnetic Q-factor, supporting its suitability for microwave component development. Notably, the integration of SRRs and ANN modeling for characterizing MD material fabrication is a pioneering effort, suggesting the potential extension of this technique to other nanoparticle-composite formulations. Thus, this approach could guide manufacturing processes to align high-frequency properties more effectively with the resulting material characterization.

REFERENCES

[1] E. Andreou, T. Zervos, A. A. Alexandridis, and G. Fikioris, "Magnetodielectric materials in antenna design: Exploring the potentials for reconfigurability," *IEEE Antennas Propag. Mag.*, vol. 61, no. 1, pp. 29–40, Feb. 2019, doi: 10.1109/MAP.2018.2883029.

[2] Y. G. Adhiyoga, S. F. Rahman, C. Apriono, and E. T. Rahardjo, "Miniaturized 5G antenna with enhanced gain by using stacked structure of split-ring resonator array and magneto-dielectric composite material," *IEEE Access*, vol. 10, pp. 35876–35887, 2022, doi: 10.1109/ACCESS.2022.3163285.

[3] G. C. Wan, J. Zhang, J. H. Zhou, X. F. Yin, and M. S. Tong, "Electromagnetic analysis of tunable bandpass filters with a magnetodielectric perturber," in *Proc. IEEE Antennas Propag. Soc. Int. Symp. (APSURSI)*, Jul. 2014, pp. 1397–1398.

[4] M. S. Tong and C. X. Yang, "VSIE-based scattering parameter analysis for a tunable bandpass filter with a PET-controlled magnetodielectric perturber," *IEEE Trans. Compon., Packag., Manuf. Technol.*, vol. 5, no. 5, pp. 661–667, May 2015, doi: 10.1109/TCPMT.2015.2426656.

[5] H. Wang, L. Zheng, H. Qin, and Z. Ying, "The design of ferrite film phase shifter," in *Proc. 4th IEEE Int. Symp. Microw., Antenna, Propag. EMC Technol. Wireless Commun.*, Nov. 2011, pp. 317–319, doi: 10.1109/MAPE.2011.6156232.

[6] K. V. Lemberg and A. M. Serzhantov, "Tunable resonant microstrip phase shifter with the magneto dielectric substrate," in *Proc. Int. Siberian Conf. Control Commun. (SIBCON)*, Sep. 2011, pp. 212–214.

[7] Y. Xiang, J. Huang, L. Fu, Y. Chen, W. Gu, and Y. Wu, "A folded substrate integrated waveguide re-entrant cavity for full characterization of magneto-dielectric powder materials," *IEEE Sensors J.*, vol. 21, no. 9, pp. 10657–10666, May 2021, doi: 10.1109/JSEN.2021.3063518.

[8] H. Sun et al., "Symmetric coplanar waveguide sensor loaded with interdigital capacitor for permittivity characterization," *Int. J. RF Microw. Comput.-Aided Eng.*, vol. 30, no. 1, Jan. 2020, Art. no. e22023, doi: 10.1002/mmce.22023.

[9] C. Yang and J.-G. Ma, "Direct extraction of complex permittivity and permeability of materials on a known-substrate from transmission/reflection measurements," *IEEE Microw. Wireless Compon. Lett.*, vol. 29, no. 10, pp. 693–695, Oct. 2019, doi: 10.1109/LMWC.2019.2933350.

[10] M. Saadat-Safa, V. Nayyeri, M. Khanjarian, M. Soleimani, and O. M. Ramahi, "A CSRR-based sensor for full characterization of magneto-dielectric materials," *IEEE Trans. Microw. Theory Techn.*, vol. 67, no. 2, pp. 806–814, Feb. 2019, doi: 10.1109/TMTT.2018.2882826.

[11] K. T. M. Shafi, M. A. H. Ansari, A. K. Jha, and M. J. Akhtar, "Design of SRR-based microwave sensor for characterization of magnetodielectric substrates," *IEEE Microw. Wireless Compon. Lett.*, vol. 27, no. 5, pp. 524–526, May 2017, doi: 10.1109/LMWC.2017.2690873.

[12] H.-Y. Gan, L.-Q. Li, W.-S. Zhao, D.-W. Wang, and G. Wang, "An improved differential CSRR-based sensor for characterizing the magneto-dielectric materials," in *IEEE MTT-S Int. Microw. Symp. Dig.*, Dec. 2020, pp. 1–3, doi: 10.1109/NEMO49486.2020.9343571.

[13] H.-Y. Gan et al., "A CSRR-loaded planar sensor for simultaneously measuring permittivity and permeability," *IEEE Microw. Wireless Compon. Lett.*, vol. 30, no. 2, pp. 219–221, Feb. 2020.

[14] S. P. Chakyar, S. K. Simon, C. Bindu, J. Andrews, and V. P. Joseph, "Complex permittivity measurement using metamaterial split ring resonators," *J. Appl. Phys.*, vol. 121, no. 5, Feb. 2017, Art. no. 054101, doi: 10.1063/1.4975111.

[15] *Skyspring Nanopowder and Nanoparticles*. Accessed: Jan. 2, 2024. [Online]. Available: https://ssnano.com/home

[16] C. Velez et al., "Investigation of ferromagnetic resonance shift in screen-printed barium ferrite/samarium cobalt composites," *IEEE Trans. Microw. Theory Techn.*, vol. 67, no. 8, pp. 3230–3236, Aug. 2019, doi: 10.1109/TMTT.2019.2927216.

[17] J. Castro, C. Morales, T. Weller, J. Wang, and H. Srikanth, "Synthesis and characterization of low-loss Fe_3O_4-PDMS magneto-dielectric polymer nanocomposites for RF applications," in *Proc. WAMICON*, Jun. 2014, pp. 1–5, doi: 10.1109/WAMICON.2014.6857768.

[18] C. S. Smith, R. Bowrothu, Y. Wang, F. Herrault, Y. K. Yoon, and D. P. Arnold, "Screen-printable, self-biased SrM/PDMS composites for integrated magnetic microwave devices," *IEEE Trans. Magn.*, vol. 57, no. 10, pp. 1–5, Oct. 2021, doi: 10.1109/TMAG.2021.3104468.

[19] L. K. Varga, "Soft magnetic nanocomposites for high-frequency and high-temperature applications," *J. Magn. Magn. Mater.*, vol. 316, no. 2, pp. 442–447, Sep. 2007, doi: 10.1016/j.jmmm.2007.03.180.

[20] L. Suriyasena Liyanage et al., "Broadband electromagnetic properties of engineered flexible absorber materials," *Adv. Mater. Technol.*, vol. 8, no. 19, Oct. 2023, Art. no. 2300887, doi: 10.1002/admt.202300887.

[21] L. F. Chen, C. K. Ong, C. P. Neo, V. V. Varadan, and V. K. Varadan, *Microwave Electronics: Measurement and Materials Characterization*, 1st ed. Hoboken, NJ, USA: Wiley, 2004.

[22] *RO4003CTM Laminates*. Accessed: Aug. 24, 2023. [Online]. Available: https://www.rogerscorp.com/advanced-electronics-solutions/ro4000-series-laminates/ro4003c-laminates

[23] H. Lobato-Morales, R. Chávez-Pérez, and J. L. Medina-Monroy, "Leaky-wave antennas based on open-plates and defected-ground open-rings with omnidirectional radiation," *J. Electromagn. Waves Appl.*, vol. 30, no. 12, pp. 1574–1590, Aug. 2016, doi: 10.1080/09205071.2016.1206839.

[24] C. Vittoria, *Magnetics, Dielectrics, and Wave Propagation With MATLAB Codes*. Boca Raton, FL, USA: CRC Press, 2010, doi: 10.1201/b17374.

[25] J. M. Drozd and W. T. Joines, "Determining Q using S parameter data," *IEEE Trans. Microw. Theory Techn.*, vol. 44, no. 11, pp. 2123–2127, Sep. 1996, doi: 10.1109/22.543972.

[26] K. T. Muhammed Shafi, A. K. Jha, and M. J. Akhtar, "Improved planar resonant RF sensor for retrieval of permittivity and permeability of materials," *IEEE Sensors J.*, vol. 17, no. 17, pp. 5479–5486, Sep. 2017, doi: 10.1109/JSEN.2017.2724942.